LABORATORY AND FIELD EVALUATION OF THE NUBISCOPE

Wiel Wauben[1], Fred Bosveld[2], Henk Klein Baltink[2]

[1] R&D Information and Observation Technology, [2] Regional Climate Department

Royal Netherlands Meteorological Institute (KNMI)

P.O. Box 201, 3730 AE De Bilt, The Netherlands

Tel. +31-30-2206 482, Fax +31-30-2210 407, e-mail: Wiel.Wauben@knmi.nl

ABSTRACT

The Royal Netherlands Meteorological Institute (KNMI) evaluated the usefulness of the NubiScope, a scanning pyrometer, for cloud observations. The NubiScope is a passive remote sensing instrument which consists of a pyrometer mounted on a pan and tilt unit. The pyrometer measures the brightness temperatures in the atmospheric thermal infrared window (8-14 µm). The NubiScope operates fully automated and performs a scan of the entire hemisphere every 10 minutes including 2 surface temperature measurements. The observed temperatures are processed to derive the obscuration type (fog, precipitation, clouds) and cloud characteristics (cloud cover, layering and altitude). During a one year field experiment at the Cabauw Experimental Site for Atmospheric Research [CESAR] the stability and the sensitivity of the pyrometer to contamination has been monitored by repeated laboratory measurements against a black body radiator. The field measurements of temperature have also been analyzed and compared with other measurements.

The NubiScope cloud product has been evaluated by observers at Rotterdam airport (at 25 km distance) using a near real-time access to the 10-minute NubiScope results, the automated ceilometer cloud product and total sky imager data. The evaluation showed that the observed differences between NubiScope and ceilometer could mostly be attributed to the better spatial representativeness of the NubiScope. Furthermore, the sensitivity of the NubiScope for high clouds is often better. Over a one year period the total cloud cover of NubiScope and ceilometer gave 44 % of the time identical results and 80 % and 87 % the differences are within ±1 and ±2 okta, respectively. The averaged difference in total cloud cover is 0.07 okta and mean absolute deviation is 1.03 okta. These differences between NubiScope and ceilometer are similar to the differences between an observer and a ceilometer. Scanning enables the NubiScope to detect isolated clouds in clear sky situations or gaps in overcast situations. This reduces the number of occurrences of 0 and 8 okta for the NubiScope as compared to a ceilometer and is in better agreement with human observed distributions. As a result of this investigation the Climate department of KNMI decided to keep the NubiScope permanently at CESAR. The Weather department confirmed the added value of the NubiScope for cloud cover observations, but for applications such as aviation the cloud height information is crucial. The combination of NubiScope cloud cover information with accurate height information requires further research.

1. INTRODUCTION

The Royal Netherlands Meteorological Institute (KNMI) uses ceilometers in combination with an algorithm to generate automated cloud reports. Since November 2002 all synoptic cloud reports in the Netherlands are generated automatically using this method (cf. Wauben, 2002). More recently, the aeronautical cloud observations at regional airports have been automated as well. Currently KNMI employs observers for aeronautic observations only at the international airports of Amsterdam and Rotterdam. Advantages of the automated cloud observations are that they are cheaper, objective, consistent, and have a higher spatial density and temporal resolution than the former human observations. Automated cloud observations are generated at about 30 locations in the Dutch meteorological network and are centrally available every 10 minutes. Cloud ceilometers can by now be considered as a part of the standard meteorological instrumentation, either as an aid for the observer for the determination of cloud base height or as a part of a fully automated weather observation system. Ceilometers are commercially of the shelf instruments that can be operated continuously and require little maintenance. Ceilometers are generally easy to use, but the detection of high cirrus clouds is still problematic due to the limited sensitivity of ceilometers. Also the detection of the cloud base during precipitation remains a challenge since precipitation masks the signature of the cloud base in the backscatter profile. Sometimes medium and low clouds can also be missed or falsely reported by the ceilometer as compared to a human observer when the cloud or moist layer is near the visual detection threshold. The verification of the performance of a ceilometer against a well defined cloud

base, or using either a hard target or a cloud simulator only ensures the correct operation of the instrument. These tests can, however, not be considered a verification of the absolute calibration, although a ceilometer generally monitors and adjusts the power output of the laser and the sensitivity of the receiver. Comparisons showed some differences in characteristics of automated and human cloud observations. Overall the users have accepted the automated cloud observations. However, large differences can occur in certain situations which are a concern for specific applications. A major limitation of the automated cloud observations using ceilometers is the lack of spatial representativeness (cf. Wauben et al., 2006). For that purpose KNMI purchased a scanning pyrometer, the so-called NubiScope, in order to evaluate it's usefulness for cloud observations.

2. NUBISCOPE

In 2008 a NubiScope was purchased and installed at the Basic Surface Radiation Network (BSRN) site of the Cabauw Experimental Site for Atmospheric Research (CESAR, 51°58'N, 4°55'E) (cf. Figure 1). The NubiScope is a passive remote sensing instrument which consists of a pyrometer mounted on a pan-and-tilt unit (PTU). The NubiScope utilizes a KT15.82 IIP pyrometer of Heitronics which is sensitive in the 8-14 µm thermal infrared window of the Earth's atmosphere and has a field of view of about 3 °. The measurement range of the pyrometer is between -100 and +350 °C, but the NubiScope limits the observed brightness temperatures to -65 °C and the factory calibration only covers temperatures above -10 °C. The NubiScope operates fully automated and performs a scan of the entire hemisphere every 10 minutes which takes about 6½ minutes. The NubiScope measures the sky temperature at 36 azimuth angles (5 ° to 355 ° in steps of 10 °) alternating between upward and downward zenith scans at 30 zenith angles (1.5 ° to 88.5 ° in steps of 3 °). The observed temperatures are processed to derive the obscuration type (fog, precipitation, clouds) and cloud characteristics (cloud cover, layering and altitude). Due to the duration of the scan a discontinuity in the sky temperatures and cloud mask can sometimes be observed in the North direction (cf. Figure 1, bottom panels). In addition the NubiScope also measures 2 surface temperatures at a nadir angle of 45 ° in the East and West direction.

The NubiScope detects clouds when the atmospheric brightness temperature is above the clear sky background values. Since NubiScope operates in the thermal infrared and scans the entire sky the cloudiness can be obtained 24 hours a day and includes spatial information of the distribution of clouds over the sky. Therefore the NubiScope has a potential added value to automated cloud observations by using time series of cloud base ceilometers which are lacking the spatial representativeness of the human cloud observations (cf. Wauben, 2006).

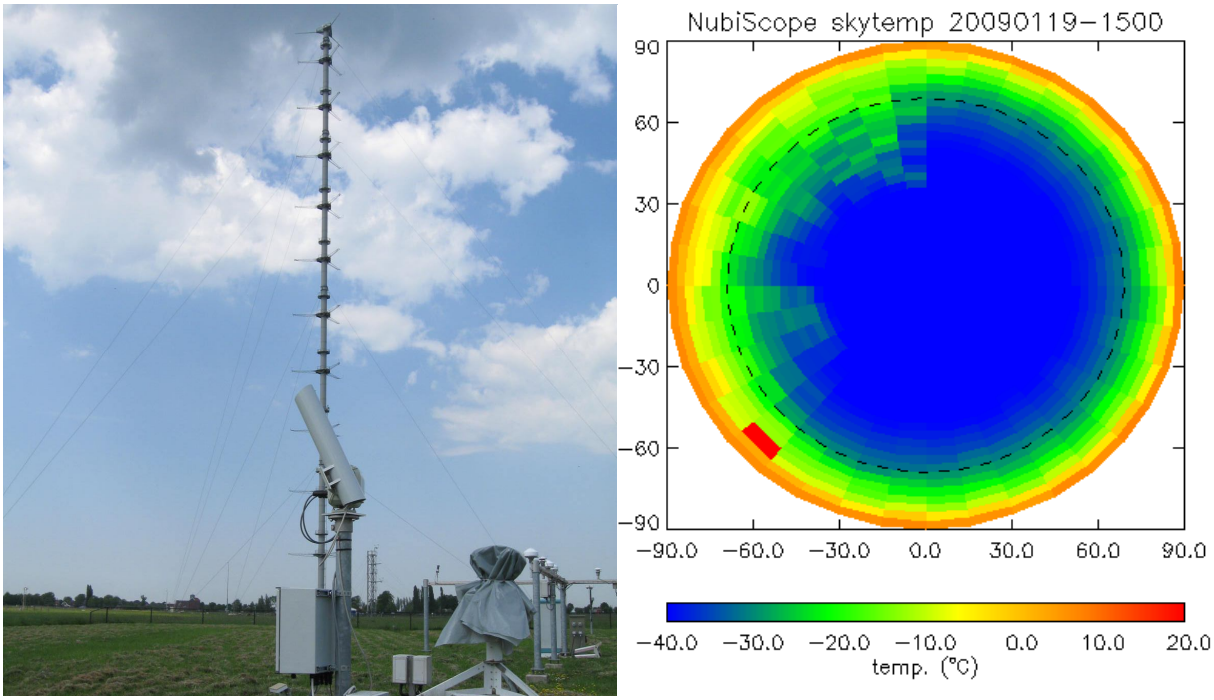

Figure 1: The NubiScope installed at the BSRN site of Cabauw (top left), the observed sky temperature during clear sky (top right), and the observed temperature (bottom right) and derived cloud mask (bottom left) during a situation with partial cloudiness.

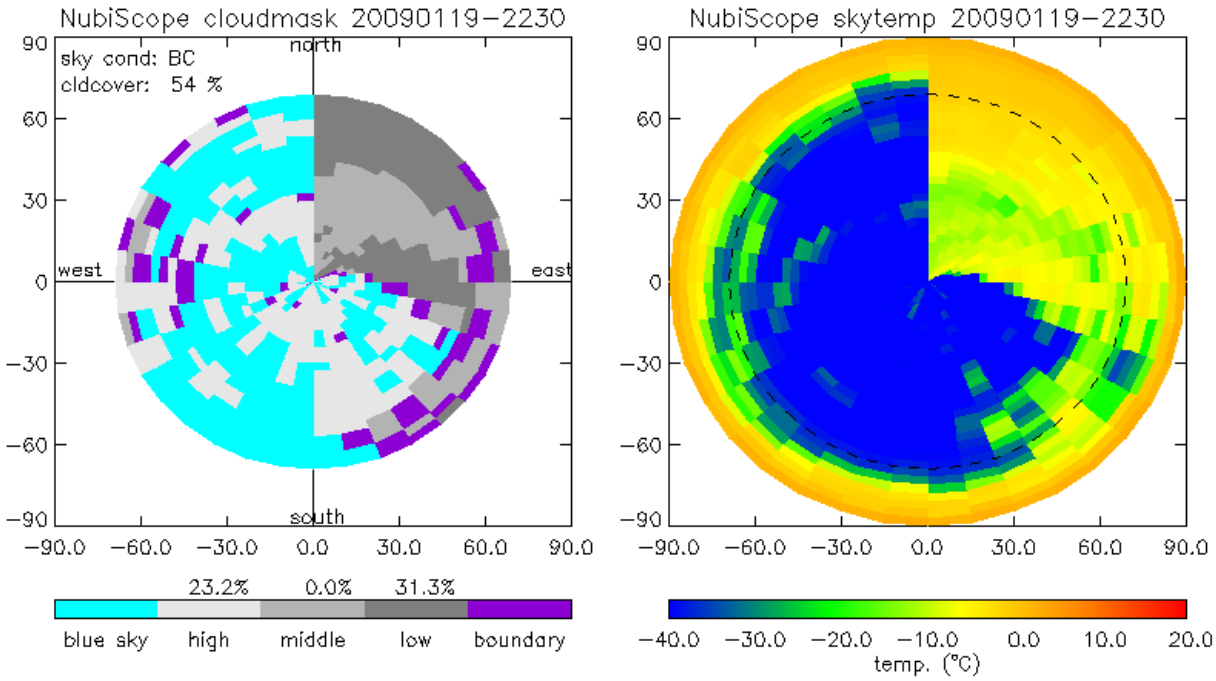

Figure 1: Continued.

In the 8-14 µm window there is a contribution of water vapor to the measured brightness temperature. Hence the clear sky brightness temperature varies over time and also increases with larger zenith angles, due to the increasing slant path through the atmosphere. To take these changes into account the NubiScope adapts the clear sky reference dynamically during each scan when sufficient cloud free scenes at various elevations are available (see. e.g. Collet et al., 2009). The zenith angle dependence of the clear sky reference temperature is described by a second order polynomial where T_{blue} denotes the clear sky reference temperature in the zenith. The effect of water vapor can be observed as the gradual increase of the observed clear sky temperature with zenith angle (cf. Figure 1). An absolute calibration of the NubiScope is not required for cloud detection, although the effect of water vapor and contamination of the lens of the pyrometer may lead to a reduced sensitivity to thin cold clouds. The absolute temperature is however required in the determination of the cloud base height. Although uncertainties associated to the relatively large field of view of the pyrometer which results in an averaging of the observed sky scene, the presence of semi-transparent cloud layers, the contribution of water vapor, and uncertainties in the actual temperature profile make the cloud base height determination of the NubiScope rather uncertain.

The NubiScope brightness temperatures near the horizon are used to estimate the ambient temperature $T_{zero.}$ The measurements at low elevations are also used to discriminate between cloudiness and fog. A NubiScope scan covers the whole sky from zenith to horizon, but the cloud determination is only performed for zenith angles <70 ° since at low elevations the sky temperatures are affected by water vapour. The NubiScope generates a cloud mask containing 828 pixels at 23 zenith angles (1.5 ° to 67.5 ° in steps of 3 °) and 36 azimuth angles. The mask can have 5 different values where 0 indicates clear sky; 1 indicates high clouds; 2 indicates medium clouds; 3 indicates low clouds; and 4 denotes a margin case. The distinction between low, medium and high cloud is made by the NubiScope by comparing the measured cloud temperature with a temperature profile with fixed vertical shape that is adjusted to the zero temperature that serves as the ambient temperature. The lower boundaries for medium and high clouds are 2100 and 5400 m respectively.

Apart form the cloud mask output the NubiScope also reports the total cloud cover and the fraction of low middle and high clouds in the so-called “Results” file together with their respective cloud base temperature and estimated cloud base height. Whereas the cloud mask is a first guess cloud product the data in the Results file are based on a more sophisticated calculation that can change the cloud discrimination of individual cloud mask pixels and also utilizes sub-pixel cloud fractions and combined scenes of low, middle and high cloud layers as well as partially clouded scenes. Furthermore the cloud cover reported in the Results file uses a zenith angle and situation dependent weighting factors that have been derived empirically in order to get an optimal correspondence with observer's practices for reporting clouds. Generally the total cloud cover reported by the NubiScope in percentage in the Results file is used directly. However in case of a sky classification of fog, precipitation or cirrus no cloudiness is reported by the NubiScope. In our evaluation fog and precipitation are treated as overcast, i.e. cloudiness of 100 % or 8 okta. In case of cirrus

the cloud mask output is used to determine the cloudiness as the percentage of the cloud mask pixels with a cloud. Finally the NubiScope also classifies each scan with one of the following the sky conditions:

CS	clear sky
CI	cirrus only
BC	broken clouds
OC	overcast
IU	identification unknown
LF	light fog
DF	dense fog
HP	heavy precipitation
TC	transparent clouds
LT	low transparent clouds

Preliminary short-term evaluations of the NubiScope have already been performed by KNMI (Wauben, 2006) and other institutes such as Meteo Swiss, DWD (cf. Feister et al., 2010), and NOAA-NWS. The purpose of this report is twofold. Firstly the stability and the effect of contamination of the pyrometer are investigated by laboratory measurements against a black surface. Secondly the NubiScope measurements for both temperature and cloudiness during a one year field test are evaluated. Full details of the laboratory and field evaluation of temperature and cloudiness are reported in a KNMI technical report (Wauben et al., 2010b).

2. LABORATORY TEMPERATURE MEASUREMENTS

The stability and the effect of contamination on the measurements of the pyrometer have been monitored in the calibration laboratory of KNMI. Prior to the installation at Cabauw the pyrometer was checked against a black body radiator. The laboratory measurements were repeated on a monthly basis, and after six months every 2 months. This section describes the measurement procedure and the results of the laboratory measurements. The aim is to verify whether the NubiScope meets the maintenance interval and accuracy requirements of 6 months and ±1°C for cloud measurements and ±0.1°C for surface temperature measurements.

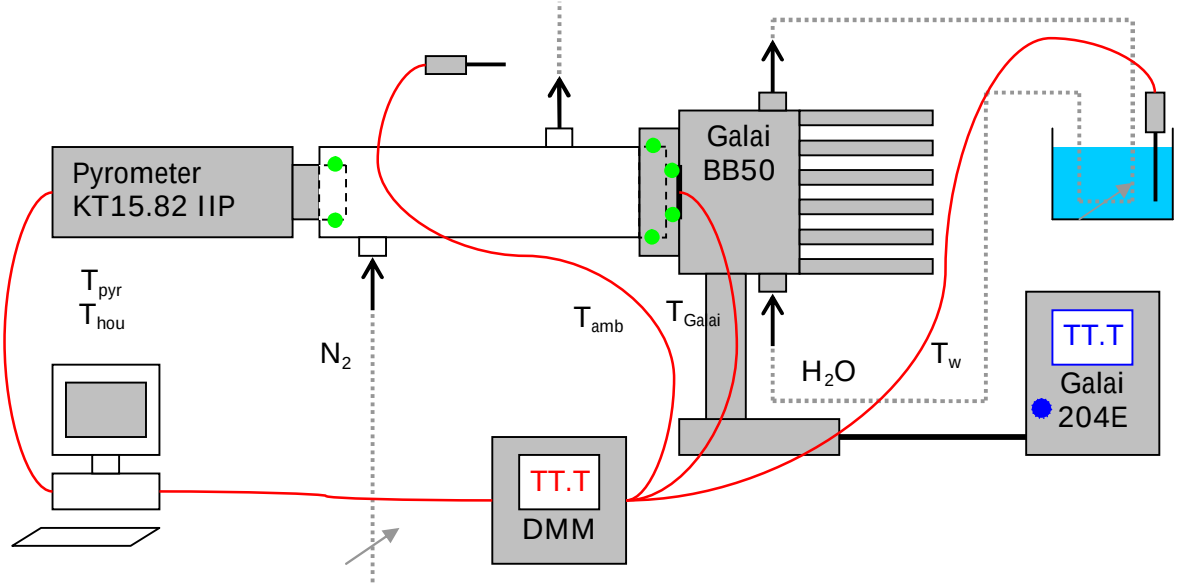

Figure 2: A schematic representation of the laboratory setup used for the monitoring of the pyrometer versus a black body radiator.

Figure 2 gives an overview of the measurement setup. The measurement setup consists of a Galai BB 50 black body with Galai 204E temperature controller, a refrigerated water bath that is used for the additional cooling of the Peltier element of the Galai black body with water, and a Digital Multi Meter. Icing or condensation must be avoided during the measurements of the pyrometer against the black body radiator at temperatures below the ambient temperature. Therefore a tube was constructed that can be mounted with rubber sealing rings between the pyrometer and the black body radiator. The tube is flushed with nitrogen with a flow rate of 0.5 l/min. The rubber sealing rings are indicated in Figure 2 by pairs of green dots. The calibration laboratory is air conditioned around 20 °C. The temperature of the cooling water T_w, the ambient temperature T_{amb} and the temperature of the black body radiator surface T_{Galai} are measured via the Digital Multi Meter, whereas the object and housing temperature of the pyrometer, T_{pyr} and T_{hou}, respectively, are

directly acquired by the measurement PC. The Galai BB 50 is a thermo-electric black body radiator with a range of -20 to 100 °C. The temperature of the black body radiator surface is monitored by a Pt-100 element with stability better than ±0.1 °C. The minimum temperature of the black body depends on the ambient temperature and can be lowered by cooling the Peltier element with water. Tests showed a stable Galai temperature just below -40 °C could be reached by using cooling water of 4 °C with a flow rate of 5 l/hour. For temperatures in the range -10 to 40 °C this additional cooling is not required. The Galai was purchased by KNMI around 1986. The last calibration of the Galai dates from 1996, when the Galai proved to be within ±0.1 °C of the reference for the entire temperature range -40 tot 100 °C with a stability and reproducibility better than ±0.05 °C and a stabilization time of at most 10 minutes. However, since the calibration was more than 10 years ago the Galai cannot be used as an absolute reference anymore. Furthermore, the coating of the black body radiator surface was damaged and dirty. The surface was cleaned with alcohol prior to the measurements. Tetenal flat black camera lacquer E-spray 200 with an emissivity of 96 % in the 8-14 µm window was obtained form Heitronics and applied to the black body radiator surface.

The NubiScope was installed at Cabauw on May 13, 2008. On June 12, 2008 the pyrometer was taken back to the calibration facilities at KNMI, thoroughly cleaned and measured against the Galai black body radiator. For each measurement the Galai black body reference temperature was varied from -40 °C and +40 °C with steps of 10 °C and back. The reproducibility of the laboratory measurements is expected to be within ±0.1 °C for Galai reference temperatures of +10 °C and higher and increases slightly to about ±0.2 °C at -40 °C. The laboratory measurements of June 12th 2008 with a clean pyrometer lens serves as the zero measurement for the field test. When relative differences are considered a second order polynomial fit to the temperature dependence of the clean reference is subtracted from the other measurements. Figure 3 and Figure 4 show the evolution of the differences between the object temperature and the Galai black body temperature with time. Figure 3 shows the measured differences between the pyrometer object temperature and the Galai black body temperature, whereas Figure 4 shows the changes in these differences with respect to the June 12th, 2008 results. Figure 4 also includes linear fits to the relative differences in order to visualize the evolution of the differences more clearly. The effect of contamination leads to an increase of the pyrometer object temperature at low reference temperatures and a reduction at high reference temperatures. The relative differences vary almost linearly with temperature. The results for the upward and downward reference temperature run for measurement series show generally good agreement, i.e. within ±0.1°C for high Galai reference temperatures to about ±0.2 °C at -40 °C and are in agreement with the expected reproducibility. Only the measurements in March 2009 show a larger deviation between -30 °C and -10 °C with the upward measurements series giving lower differences. The reason for these large differences is unclear.

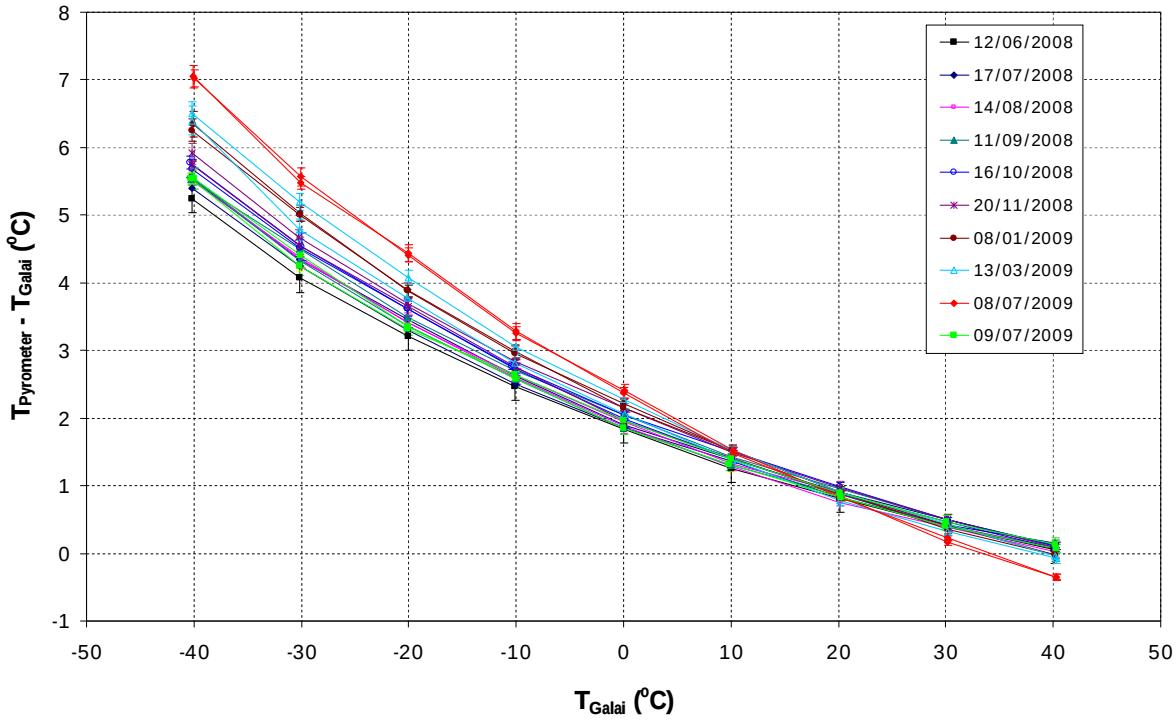

Figure 3: Differences between the pyrometer object temperature and the Galai black body temperature as a function of the Galai reference temperatures at various moments during the field test.

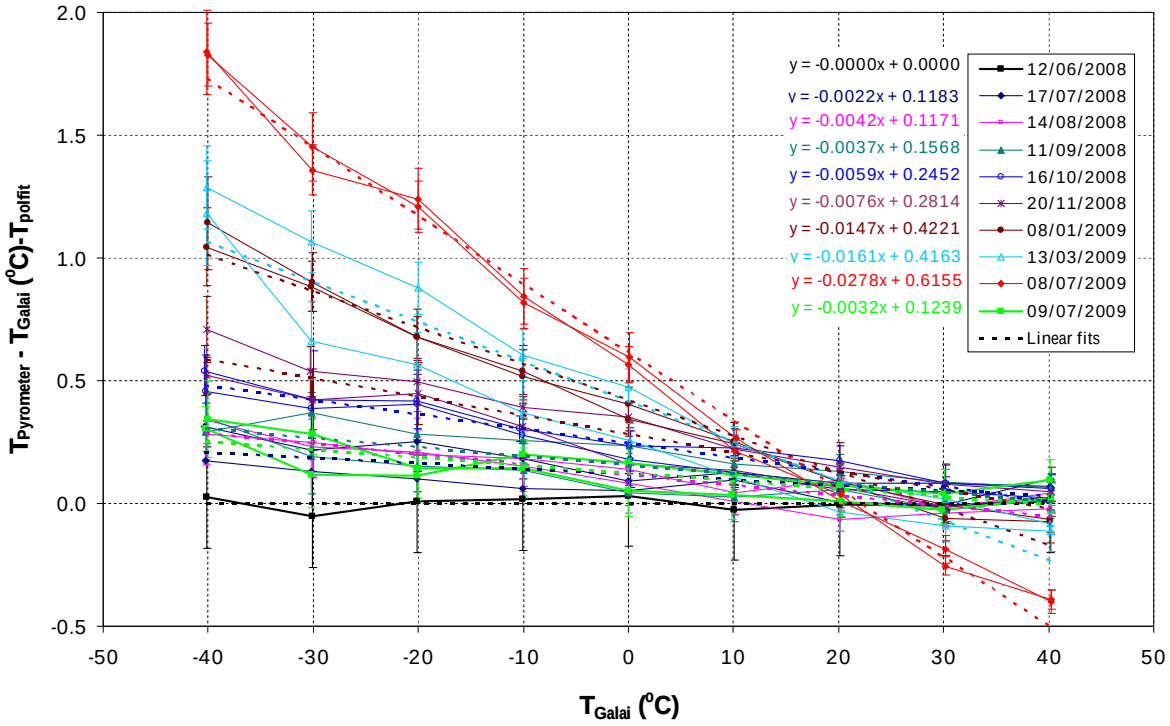

Figure 4: The differences between the pyrometer object temperature and the Galai black body temperature with respect to the zero reference as a function of the Galai reference temperatures.

After a year in the field the differences increased to about +1.8 °C at -40 °C and -0.4 °C at +40 °C. The curves show a gradual increase of the deviation from the zero reference over time. The deviations for a reference temperature of -40 °C increased to about 0.5 °C after 4 months, 1.0 °C after 6 months and 2.0 °C after 12 months. However, it is not clear if this trend for contamination is typical and whether it is affected by contamination events. Also note that the pan and tilt unit showed occasional problems that left the NubiScope more exposed looking upwards whereas normally it measures the entire sky in about 6 minutes after which it returns to its home position (horizon, North). In March 2009 the PTU broke down and was eventually replaced by a new unit which resulted in only 5 measurement days in that particular month.

The pyrometer with a clean lens was also measured against the black body on several occasions prior, during and after the field test. Figure 5 shows the temperature differences between black body and pyrometer with a clean lens obtained on these occasions. The field test was completed in October 2009 and the differences at June 2008, July 2009 and October 2009 show a slight increasing trend. In November 2009 the pyrometer was send to Heitronics for a check and recalibration and after return a large difference can be observed. Note that the previous calibration of the pyrometer was performed on November 7, 2007 when the pyrometer was purchased by the manufacturer of the NubiScope. During these 2 years the absolute calibration of the pyrometer showed differences of about +2 °C at -40 °C to -0.5 °C at +40 °C. The temperature dependence of the differences observed between the pyrometer and Galai cannot be reproduced by a suitable emissivity of the Galai surface and an emissivity of the lens. The temperature reported by the clean and newly calibrated pyrometer and black body temperature are, however, in agreement over the entire temperature range from -40 °C to +40 °C by adopting the emissivity's ε_{Galai} = 97.3 % and ε_{lens} = 0 %.

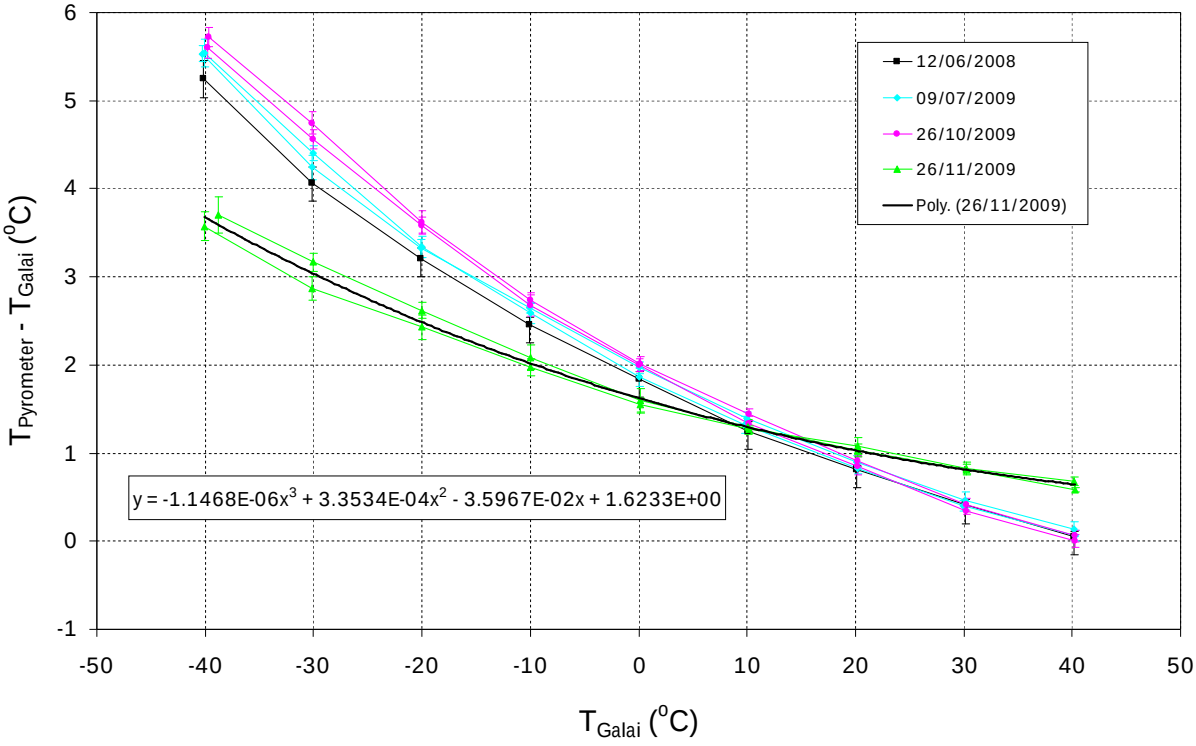

Figure 5: Differences between the pyrometer object temperature (with clean lens) and the Galai black body temperature as a function of the Galai reference temperatures at various moments during the field test.

3. FIELD TEMPERATURE MEASUREMENTS

Figure 6 shows a scatter plot of the zero temperature derived by the NubiScope from the sky temperature measurements near the horizon (T_{zero}) and the ambient temperature observed at 1.5 m ($T_{ambient}$). The filaments indicate days with pronounced differences. The measurements show a good correlation (0.968), but the zero temperature of the NubiScope shows generally lower values. The offset is -0.95 °C and the standard deviation is 1.67 °C. A histogram of the differences between zero and ambient temperature observed during the field test is given in Figure 7. The differences between zero and ambient temperature show no dependency with total cloud cover, although the lowest values (down to -15 °C) generally occur during clear sky conditions. The observed differences show a dependency on the solar zenith angle and relative humidity with on average lower values at smaller solar zenith angle and low relative humidity. The ambient temperature and relative humidity are observed at 1.5 m whereas the zero temperature is a brightness temperature observed by a slant path through the atmosphere. Hence the zero temperature also contains contributions from higher altitudes and thus in general lower temperatures. In order to investigate this effect, the ambient temperature measurement at 2, 10, 20, 40, 80, 140 and 200 m in the meteorological mast at Cabauw are considered. Some statistics are given in Table 1. The 200 m temperature has the lowest offset with the zero temperature of -0.8 °C , but the standard deviation of 2.4 °C is rather large, whereas at 10 m the standard deviation (1.6 °C) is smallest but with a slightly higher offset (-1.1 °C). However, the differences with the zero temperature show no significant improvement when using the ambient temperatures at other altitudes.

Table 1: Statistics of the differences between the NubiScope zero temperature, the ambient temperature, and temperature at various levels in the meteorological mast at Cabauw.

Temperature	*Offset*	*Std dev*	*Range*	#
Ambient 1.5 m	-0.95	1.67	20.4	57612
Mast 2 m	-0.92	1.67	20.8	57612
Mast 10 m	-1.15	1.60	20.9	57612
Mast 20 m	-1.18	1.65	21.6	57612
Mast 40 m	-1.51	1.85	23.3	57612
Mast 80 m	-1.18	1.99	23.9	57612
Mast 140 m	-0.95	2.21	24.4	57612
Mast 200 m	-0.78	2.41	25.7	57612

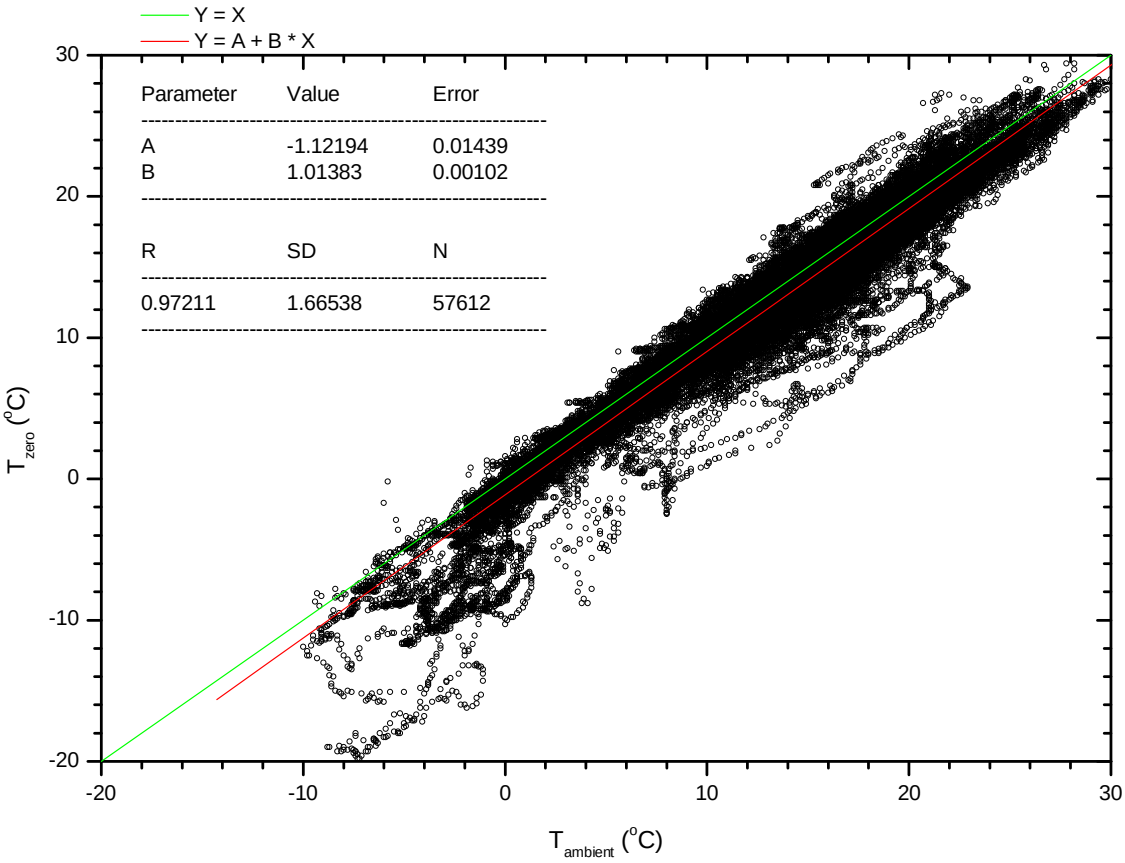

Figure 6: Scatter plot of the NubiScope zero temperature versus the ambient temperature.

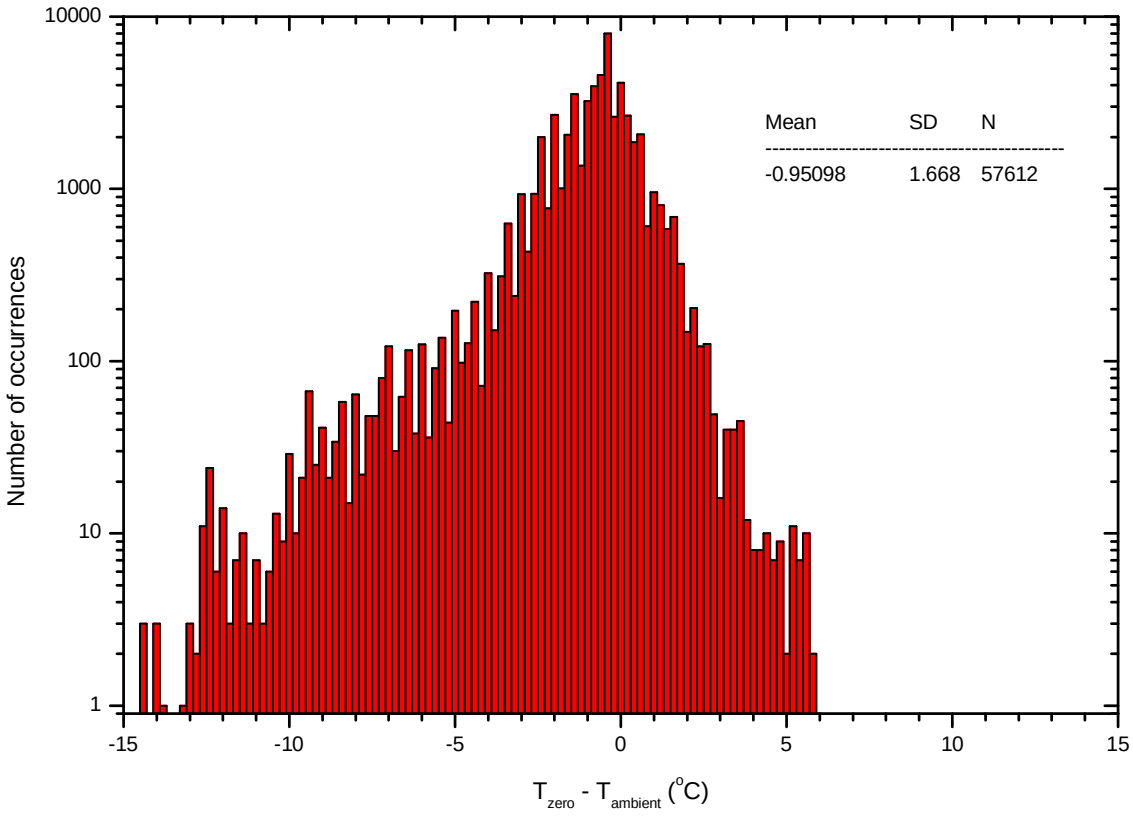

Figure 7: Histogram of the differences between zero and ambient temperature observed during the field test.

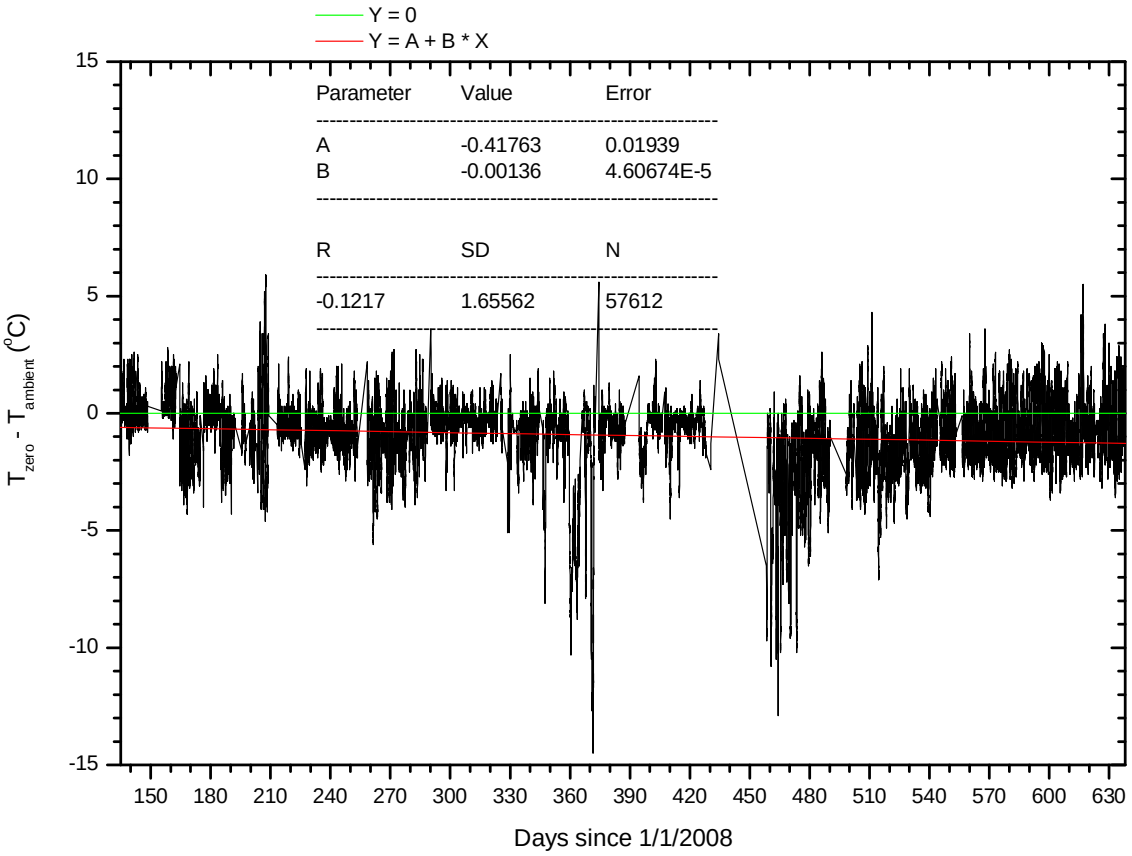

Figure 8: The differences between zero and ambient temperature observed during the field test as a function of time.

Figure 8 shows the evolution of the differences between zero and ambient temperature as a function of time. The curve shows a small negative tendency, but note that the negative values between day numbers 458 and 472 (i.e. April 3 and April 16, 2009 13 UT) occurred when the vertical alignment of the newly installed PTU was 4 ° off. Note that in clear conditions the sun can sometimes be observed (cf. Figure 1, top right panel where the red pixel in southwesterly direction indicates the solar position) Tracking the position of the sun can be used to monitor the alignment of the PTU (cf. Wauben et al., 2010b).

The zenith angle dependence of the clear sky reference temperature is described by the NubiScope as a second order polynomial where T_{blue} denotes the clear sky reference temperature in the zenith in order to account for the contribution of water vapour to the measured brightness temperatures. The clear sky reference temperature is adapted dynamically by the NubiScope if sufficient cloud free scenes at various elevations are available. In this section only those 10-minute intervals are considered where the T_{blue} reported by the NubiScope differs from the previous value. Hence only those situations are considered when T_{blue} corresponds to the measurement time. The zenith clear sky temperature correlates poorly with the relative humidity observed at 1.5 m (correlation is -0.22 and standard deviation is 10.48 °C), in fact the correlation with ambient temperature (cf. Figure 9) is much better (correlation is 0.87 and standard deviation is 3.87 °C). The poor correlation with relative humidity at 1.5 m is hardly surprising since the zenith clear sky brightness temperature consists of contributions from water vapour at all altitudes. An integrated water vapour (IVW) product that is readily available at Cabauw is derived from the delay on GPS signals. Figure 10 shows a scatter plot of the zenith clear sky temperature and the integrated water vapour derived from GPS. The correlation coefficient is 0.91 and the standard deviation of is 3.3 °C. The differences between the second order polynomial fitted to the IVW and the zenith clear sky temperature have a Gaussian distribution and the differences show only a small negative tendency over time (Figure 11).

The correlation between GPS integrated water vapour and NubiScope zenith clear sky temperature is rather good, but the differences are too large in order to be able to use the IVW to put constraints on the NubiScope zenith clear sky temperature or to monitor trends. However, the good correlation indicates that a further refinement which involves not only just IWV, but vertical profiles of humidity and temperature that are observed on site by a radiometer. Radiation transfer calculations should be used to model the expected sky brightness temperatures. This need not be restricted to clear sky conditions, but can also be considered for

situations with a homogeneous cloud deck. The latter gives also useful information on the cloud base height information derived by the NubiScope.

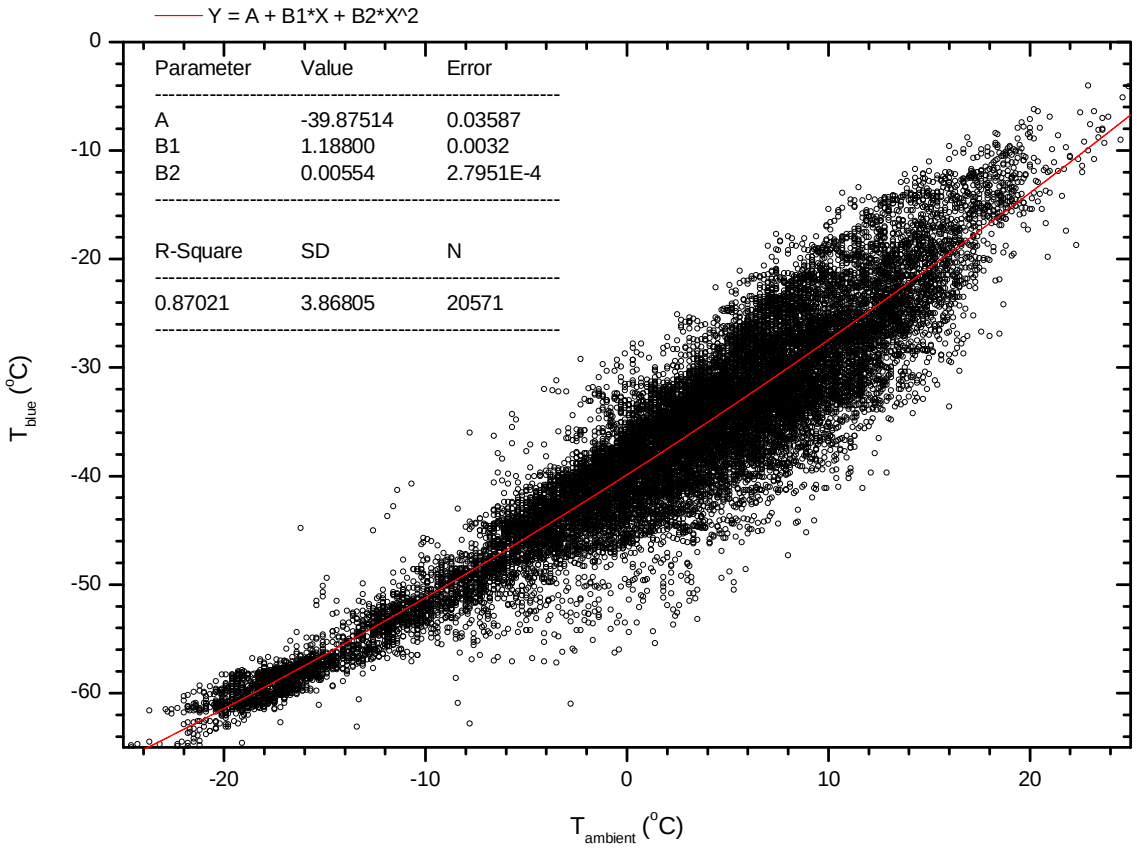

Figure 9: Scatter plot of the zenith clear sky temperature observed during the field test versus ambient temperature.

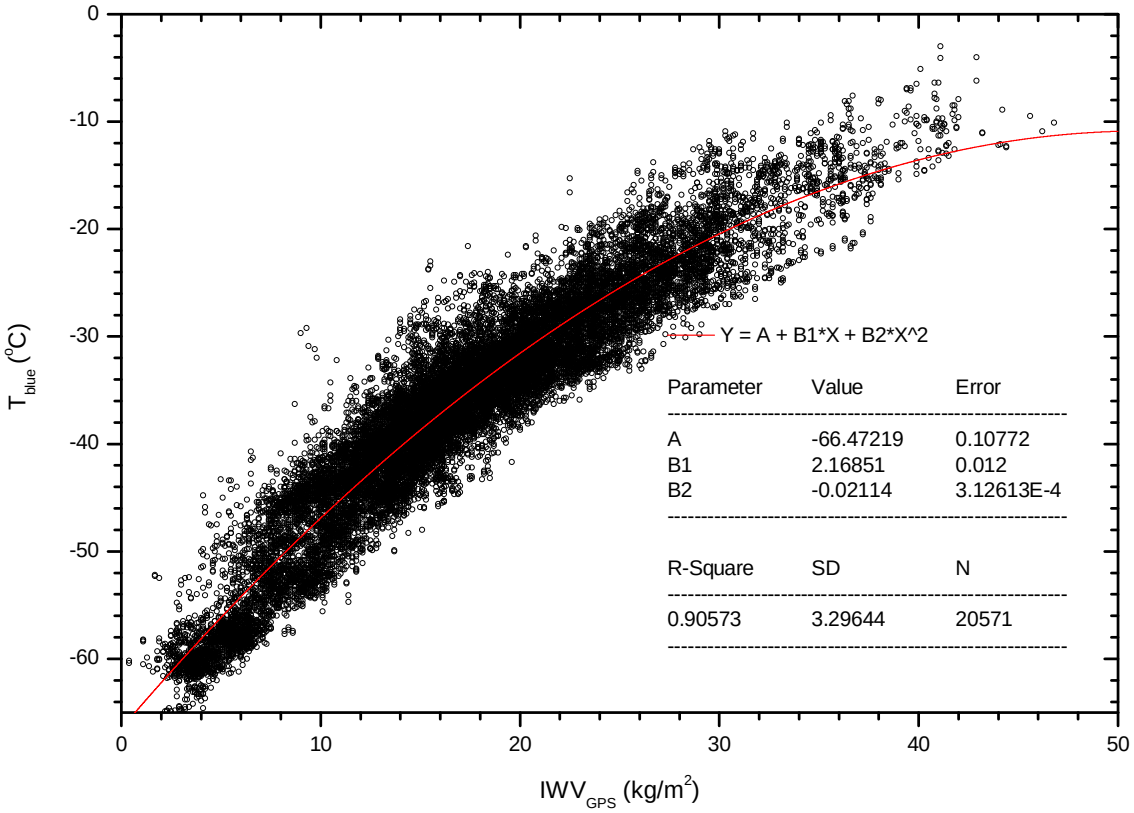

Figure 10: Scatter plot of the zenith clear sky temperature observed during the field test versus the GPS integrated water vapour column.

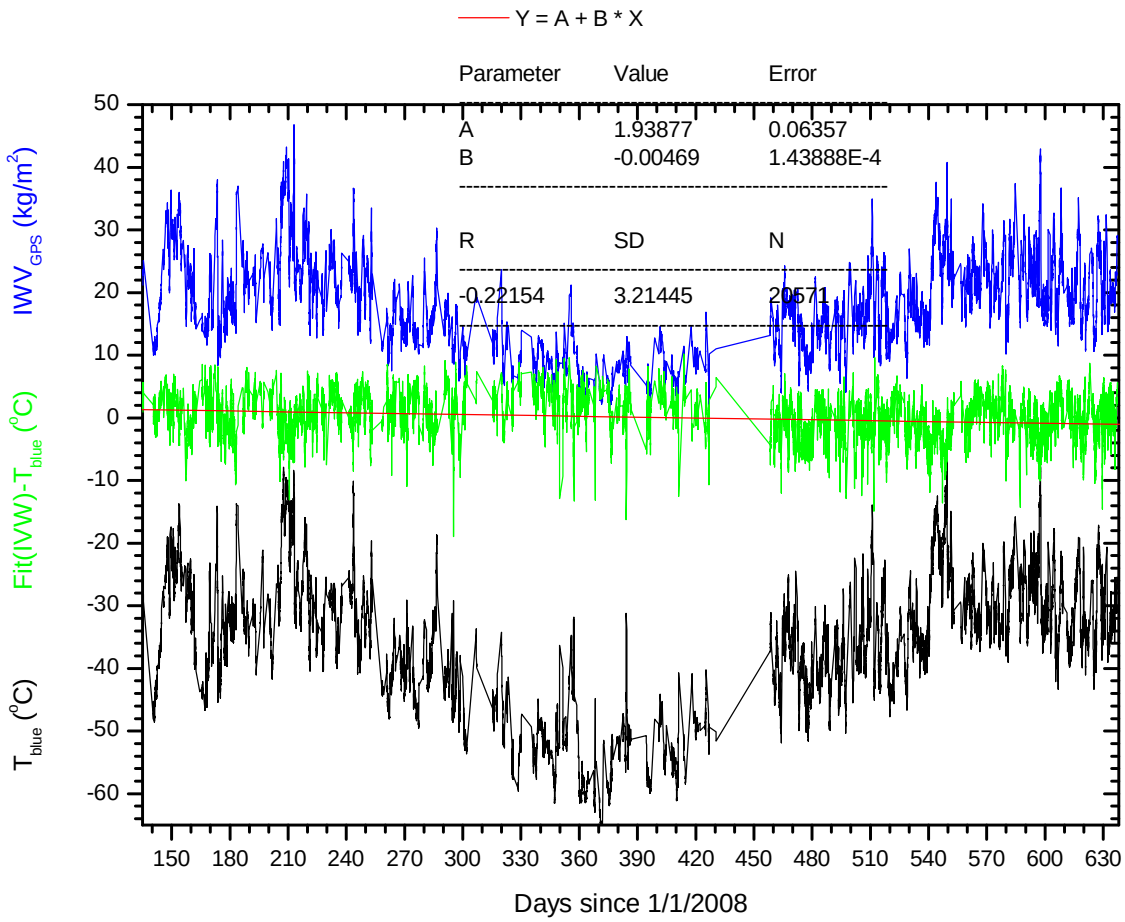

Figure 11: The zenith clear sky temperature, GPS IWV, and the differences between the second order polynomial fit to IWV and zenith clear sky temperature observed during the field test as a function of time.

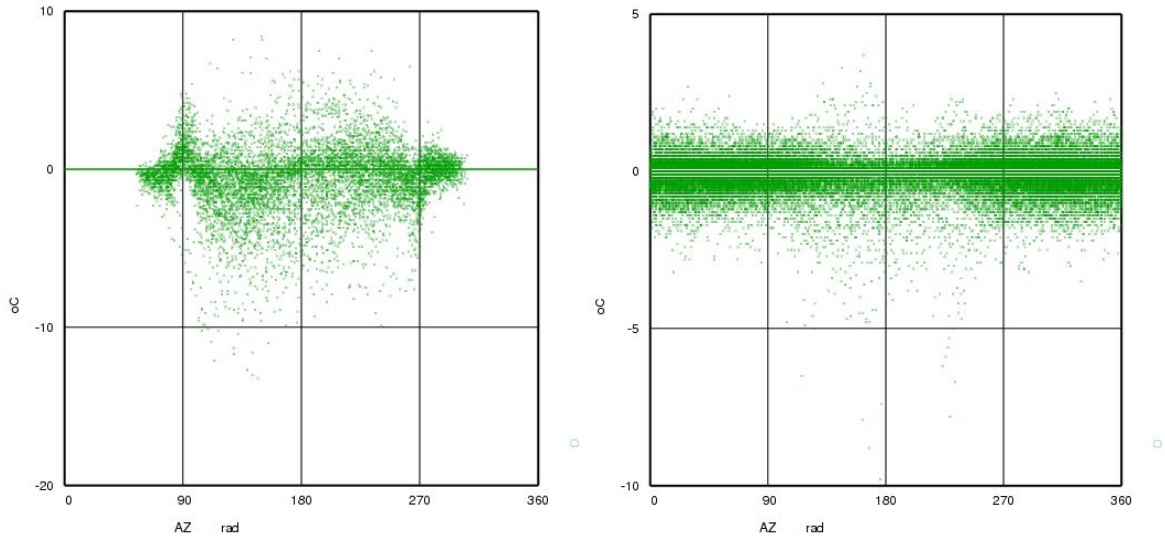

Figure 12: The differences between the West and East skin temperatures as function of solar azimuth angles with (left) and without (right) direct sunlight. Note the different vertical scale between the left and right panel.

Next the surface skin temperatures observed by the NubiScope are investigated. The differences between the West and East skin temperatures are shown as function of solar azimuth angles with and without direct sunlight in Figure 12. At azimuth around 90 ° the westward land point has higher temperature then the eastward land point. At azimuth around 270 ° the reverse occurs. This is in line with the idea that shaded and lighted patches of grass are seen by the NubiScope when the Sun is aligned along the path of the land points. Large differences up to 10 °C occur for other solar azimuth angles. These excursions are in general towards a colder westward point. When no direct sunlight is present deviations between the two land points tends to be within 1 °C, both during day and night time. When the NubiScope surface skin

temperatures are compared with those derived from an Eppley pyrgeometer, which measures broad band upwelling long wave radiation, the agreement is reasonable (correlation 0.94) without direct sunlight, but the NubiScope values are approximately 1 °C lower especially at low temperatures. This bias is evident over the whole temperature range when only night time measurements are considered. The temperature bias was investigated in situations with a snow deck while the wet bulb temperature is above zero. In these situations with melting snow the NubiScope reported skin temperature very close to 0 °C, whereas the Eppley was about 1 °C too warm. Hence we believe the NubiScope surface skin temperatures to be correct, but the small field of view and inhomogeneities in the grass affect the NubiScope surface temperatures.

4. MANUAL EVALUATION OF NUBISCOPE CLOUDINESS

The total cloud cover reported by the NubiScope and a LD40 ceilometer (using the AUTOMETAR cloud algorithm that uses 10-minutes of cloud base data) at Cabauw has been evaluated by the KNMI observers at Rotterdam airport (25 km distance from Cabauw). For that purpose the observers had near real-time access to the 10 minute data of the NubiScope (overall cloud result as well as the cloud mask), the LD40 cloud base data and total cloud cover, the meteorological data of Cabauw and remote sensing data measured at the CESAR. Particularly the images of a Total Sky Imager (TSI) where used during day time to evaluate the NubiScope and LD40 results. Whenever the situation was considered suitable, e.g. in case of cirrus, the local cloud condition at Rotterdam was used in the remote evaluation. The evaluation was performed in the period June 1, 2009 to August 25, 2009 during which the observers were asked to make an evaluation whenever the difference in the total cloud cover reported by NubiScope and LD40 exceeded ±2 okta. Whenever possible, they should indicate which sensor (if any) reported the correct cloudiness and give a possible reason for the observed differences. The evaluations were facilitated by a web tool (cf. Figure 13).

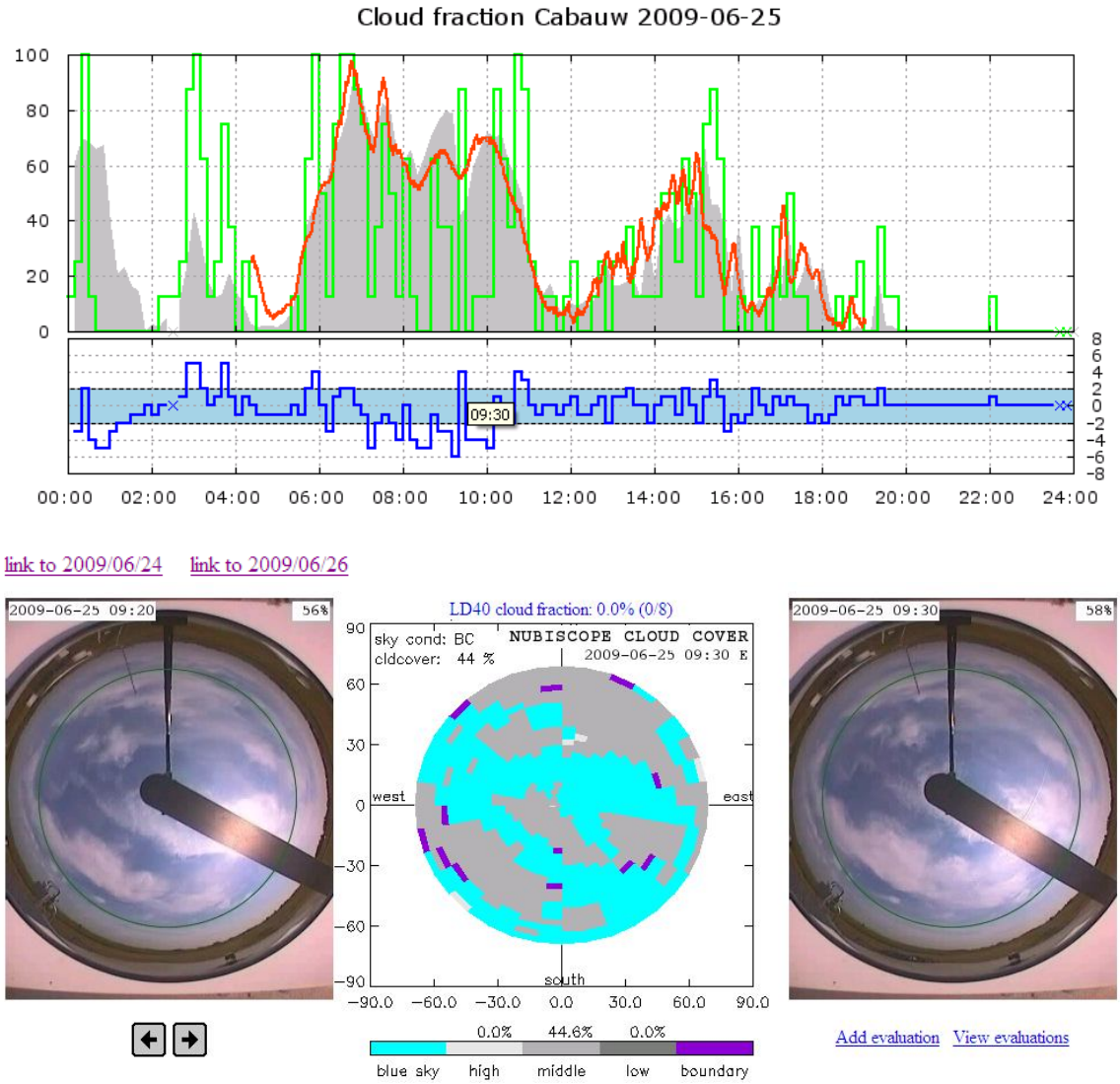

Figure 13: The NubiScope evaluation screen showing: a daily overview of the total cloud cover of NubiScope (gray), LD40 (green) and TSI (red) on June 25th, 2009 and the differences LD40-NubiScope (blue) (top); the video images of the TSI at the start and end of the NubiScope scan and the NubiScope cloud mask at 9:30UT (bottom).

Table 2: Contingency table of the total cloud cover reported by NubiScope versus LD40-METAR at Cabauw for 10-minute intervals in the period June 1, 2009 – August 25, 2009.

LD40 METAR 10min 50*12sec

Nubi	NA	0	1	2	3	4	5	6	7	8	Total	Sum	<Δn>	<|Δn|>
NA	0.02%	0.23%	0.10%	0.06%	0.09%	0.13%	0.10%	0.17%	0.63%	2.16%	3.70%	458		
0	0.15%	15.17%	2.06%	0.17%	0.05%	0.06%	0.03%	0.05%	0.04%	0.03%	17.67%	2055	0.22	0.22
1	0.41%	10.65%	5.08%	1.41%	0.82%	0.44%	0.26%	0.20%	0.22%	0.21%	19.28%	2273	-0.08	1.03
2	0.16%	1.01%	1.37%	0.84%	0.80%	0.64%	0.50%	0.36%	0.21%	0.23%	5.95%	706	0.68	1.81
3	0.19%	0.38%	0.51%	0.56%	0.75%	0.87%	0.66%	0.53%	0.76%	0.29%	5.32%	636	1.05	2.07
4	0.06%	0.21%	0.23%	0.17%	0.37%	0.53%	0.65%	0.88%	1.16%	0.63%	4.84%	566	1.27	2.21
5	0.10%	0.14%	0.17%	0.07%	0.16%	0.38%	0.50%	0.73%	1.95%	1.15%	5.26%	618	1.10	1.98
6	0.23%	0.08%	0.09%	0.09%	0.10%	0.22%	0.16%	0.40%	1.63%	2.66%	5.42%	653	0.89	1.68
7	1.17%	0.19%	0.30%	0.14%	0.27%	0.36%	0.40%	0.62%	3.32%	16.18%	21.79%	2656	0.40	1.08
8	0.77%	0.09%	0.15%	0.03%	0.11%	0.10%	0.04%	0.09%	0.73%	13.14%	14.47%	1763	-0.27	0.27
Total	3.25%	27.90%	9.96%	3.48%	3.44%	3.60%	3.22%	3.84%	10.03%	34.53%	100.0%	12384	0.34	1.03
Sum	402	3245	1161	409	407	431	383	464	1234	4248	12384			

Δn±0=	39.73%	Δn±1=	78.88%	Δn±2=	89.22%	Miss=	3.34%	False =	7.44%

Table 2 gives the contingency table of the total cloud cover reported by NubiScope and LD40 at Cabauw during the period of the manual evaluation. Table 2 gives at row "i" and column "j" the fraction of 10-minute intervals where the NubiScope reported a total cloud cover "i" okta whereas the LD40 reported "j" okta. The fraction of cases when a sensor is not available is indicated in the gray cells. Total column and row give the total fraction in each okta interval for NubiScope and LD40, respectively, excluding missing data. Below the contingency table the fraction of valid sensor data with identical cloudiness (Δn±0), i.e. on the green diagonal, is reported as well as the fraction of data within ±1 okta and ±2 okta. “Miss” denotes the fraction of valid cases in the red area, when the cloud cover reported by the LD40 is more than 2 okta lower than that of the NubiScope. “False” denotes the fraction of valid cases in the blue area, when the cloud cover reported by the LD40 is more than 2 okta higher than that of the NubiScope. Furthermore, the averaged difference in total cloud cover <Δn>=<nLD40-nNubi>, and the averaged absolute difference in total cloud cover <|Δn|> =<|nLD40-nNubi|>) are reported in okta's.

In 89 % of all 10-minute intervals during that period NubiScope and LD40 agree within ±2 okta. The 3 % and 7 % of the cases in, respectively, the Miss and False area where the NubiScope reports cloudiness more than 2 okta lower and higher than the LD40 are the cases which are considered in the manual evaluation. The scores of NubiScope versus LD40 in this almost 3 month period are similar to the scores obtained over the full period of the field evaluation of the NubiScope at Cabauw. The only difference is that during the evaluation period the LD40 does generally overestimate the cloudiness which is evident from the positive averaged difference in total cloud cover (<Δn>=<nLD40-nNubi>) and also explains the larger number of False compared to Miss cases.

Table 3: The total number of correct and faulty reports for NubiScope and LD40 during the evaluation, and assuming that no remark indicates a non faulty and hence a correct sensor observation.

	NubiScope	*LD40 (METAR)*
Correct	71	7
Faulty	28	184
Correct - Faulty	43	-177
Non Faulty	231	75
Non Faulty - Faulty	203	-109

A total of 265 manual evaluations have been made. These evaluations have been inspected individually and scores have been assigned to the NubiScope and LD40 whenever the evaluation mentioned that either instrument reported a correct or faulty total cloud cover. The sum of the scores for NubiScope and LD40 are given in Table 3. Please note that the scores only give an indication of the performance of the sensor. This is

not only related to the absence of a true reference system for cloud observations and the distance of the observer, but furthermore each evaluation is counted as 1 item whereas often the evaluation does not correspond to a single 10-minute interval. Sometimes the evaluation was not conclusive and for a few cases the evaluation was not in agreement with the data for that period. These cases are not included in Table 3. The NubiScope has more correct and less faulty evaluations than the LD40. Often a positive comment is not reported. Hence Table 3 also contains the number of non faulty sensor reports. The scores Correct - Faulty and Non Faulty - Faulty both show that the NubiScope performs better than the LD40. The main reason given for the faulty LD40 total cloud cover is the lack of spatial representativeness. Furthermore the LD40 often does not report middle and high level clouds. The NubiScope generally performs better for middle and high level clouds than the LD40, although there are also situations when the reverse occurs. In some situations the scan speed of the NubiScope (1 per 10-minutes) was considered too slow to give a representative cloud report in a rapidly changing cloud deck. A few reports mention explicitly that the cloudiness reported by the NubiScope is too slow or lagging. However, overall the scanning NubiScope gives a much better estimation of the cloudiness than LD40. Nevertheless the evaluation also contained several reports of faulty height classification by the NubiScope.

5. EVALUATION OF NUBISCOPE CLOUDINESS

The NubiScope has been installed at the Cabauw research site of KNMI since May 14, 2008 and has been operated up to the end of September 2009 at which point the NubiScope was taken indoors for replacement of the PTU and recalibration of the pyrometer by the manufacturer. Note that Boers et al. (2010) and Wauben et al. (2010a) compared the total cloud cover reported by 5 observing techniques, including the NubiScope, for a 1-year period from May 15, 2008 to May 14, 2009. In this section the NubiScope cloud observations have been compared against the automated cloud reports generated by a Vaisala LD40 ceilometer. The latter is used for the operational determination of the automated cloud reports in the KNMI observational network. For aeronautical cloud reports the cloud bases hits of the last 10-minutes are evaluated for that purpose (METAR), whereas for synoptical and climatological purposes the cloud bases hits of the last 30-minutes - where the last 10-minute have double weight - are evaluated (SYNOP, see Wauben, 2002 for details). The total cloud cover results of the NubiScope and the LD40-METAR are given as a contingency table in Table 4. The green diagonal contains 44 % of the data where LD40 and NubiScope give identical total cloud cover. The yellow and orange bands contain 80 % and 89 % of the data that is within ±1 and ±2 okta, respectively. The averaged difference in total cloud cover is 0.07 okta and mean absolute deviation is 1.03 okta. The averaged difference in total cloud cover and mean absolute deviation are also reported as a function of the NubiScope total cloud cover. The differences between the NubiScope and the LD40 are similar to the differences observed between the manual observer and the LD40 (cf. Wauben et al., 2006). As a result of scanning the NubiScope is able to detect clouds in almost clear sky situations or gaps in overcast situations. This is illustrated by the reduced number of occurrences of 0 and 8 okta for the NubiScope compared to the LD40. In fact for the NubiScope the number of 0 and 8 okta are nearly the same as for 1 and 7 okta, respectively. There is hardly a bias in the total cloud amount reported by NubiScope and LD40 and the Miss and False fractions are both 6 %. In case the evaluation period of the cloud algorithm is increased, as is the case for the SYNOP algorithm, the overall agreement between NubiScope an LD40 improves (cf. Table 5). The percentage of data within ±0, ±1 and ±2 okta, is now 46, 81, 90 %, respectively, whereas 5 % is in the Miss and False region. The averaged difference in total cloud cover and the mean absolute deviation reduce slightly and are now 0.06 and 0.95 okta, respectively. The fraction of LD40 data with 0 or 8 okta reduces by about 5 %, but it is still significantly larger than the number of 1 and 7 okta events. Note also that the fraction of cases in the 2-6 okta region increases and is larger for LD40-SYNOP (22.5 %) than for the NubiScope (19.8 %), whereas LD40-METAR (16.3 %) had less data in the 2-6 okta region than the NubiScope. The total fraction of cases per okta interval for NubiScope, LD40-METAR and LD40-SYNOP are shown in Figure 14.

Table 4: Contingency table of the total cloud cover reported by NubiScope versus LD40-METAR at Cabauw for all10-minute intervals in the period May 14, 2008 – September 30, 2009.

LD40 METAR 10min 50*12sec

Nubi	NA	0	1	2	3	4	5	6	7	8	Total	Sum	<Δn>	<|Δn|>
NA	0.21%	2.66%	1.00%	0.37%	0.33%	0.44%	0.40%	0.49%	1.57%	6.53%	14.00%	10184		
0	0.21%	11.14%	2.71%	0.44%	0.25%	0.16%	0.09%	0.08%	0.05%	0.08%	15.00%	9136	0.46	0.46
1	0.27%	8.77%	3.92%	1.04%	0.64%	0.46%	0.25%	0.15%	0.18%	0.28%	15.71%	9568	-0.01	1.10
2	0.10%	1.00%	1.09%	0.62%	0.54%	0.51%	0.34%	0.23%	0.16%	0.09%	4.59%	2796	0.39	1.74
3	0.10%	0.42%	0.49%	0.40%	0.47%	0.63%	0.50%	0.34%	0.43%	0.15%	3.83%	2335	0.65	2.03
4	0.06%	0.26%	0.26%	0.19%	0.29%	0.44%	0.46%	0.58%	0.76%	0.33%	3.57%	2172	0.76	2.15
5	0.06%	0.22%	0.18%	0.14%	0.13%	0.28%	0.37%	0.49%	1.24%	0.64%	3.68%	2241	0.59	2.07
6	0.09%	0.15%	0.15%	0.06%	0.09%	0.17%	0.23%	0.34%	1.39%	1.56%	4.13%	2516	0.44	1.75
7	0.65%	0.60%	0.59%	0.36%	0.43%	0.55%	0.64%	0.85%	4.11%	14.87%	23.01%	14016	-0.01	1.30
8	0.68%	0.30%	0.32%	0.18%	0.17%	0.21%	0.20%	0.31%	2.08%	22.72%	26.49%	16139	-0.40	0.40
Total	2.43%	22.85%	9.71%	3.43%	3.01%	3.41%	3.09%	3.37%	10.40%	40.73%	100.0%	60919	0.07	1.03
Sum	1768	13918	5914	2089	1832	2075	1885	2054	6338	24814	60919			

Δn±0=	44.13%	Δn±1=	80.25%	Δn±2=	88.66%	Miss=	5.82%	False=	5.52%

Table 5: Contingency table of the total cloud cover reported by NubiScope versus LD40-SYNOP at Cabauw for all 10-minute intervals in the period May 14, 2008 – September 30, 2009.

LD40 SYNOP 30min 30*1min

Nubi	NA	0	1	2	3	4	5	6	7	8	Total	Sum	<Δn>	<|Δn|>
NA	0.21%	2.17%	1.11%	0.50%	0.45%	0.53%	0.59%	0.72%	1.94%	5.78%	14.00%	10184		
0	0.21%	9.98%	3.52%	0.80%	0.38%	0.15%	0.05%	0.03%	0.03%	0.06%	15.00%	9136	0.53	0.53
1	0.27%	6.52%	5.01%	1.73%	1.07%	0.62%	0.32%	0.13%	0.12%	0.18%	15.71%	9569	0.20	1.03
2	0.10%	0.56%	0.98%	0.84%	0.77%	0.67%	0.42%	0.19%	0.12%	0.04%	4.59%	2797	0.62	1.54
3	0.10%	0.21%	0.42%	0.50%	0.62%	0.66%	0.60%	0.46%	0.29%	0.07%	3.84%	2336	0.73	1.75
4	0.06%	0.15%	0.22%	0.24%	0.36%	0.54%	0.65%	0.65%	0.60%	0.15%	3.56%	2171	0.62	1.81
5	0.07%	0.12%	0.17%	0.16%	0.21%	0.35%	0.55%	0.70%	1.10%	0.31%	3.68%	2240	0.36	1.73
6	0.09%	0.09%	0.12%	0.08%	0.15%	0.23%	0.40%	0.66%	1.57%	0.83%	4.13%	2517	0.11	1.46
7	0.66%	0.37%	0.50%	0.35%	0.53%	0.65%	1.02%	1.67%	5.77%	12.14%	23.00%	14009	-0.13	1.19
8	0.69%	0.19%	0.31%	0.23%	0.20%	0.22%	0.28%	0.45%	2.61%	21.99%	26.48%	16130	-0.43	0.43
Total	2.46%	18.21%	11.26%	4.94%	4.29%	4.09%	4.29%	4.94%	12.22%	35.78%	100.0%	60905	0.06	0.95
Sum	1786	11089	6856	3007	2611	2488	2610	3008	7443	21793	60905			

Δn±0=	45.97%	Δn±1=	81.13%	Δn±2=	89.98%	Miss=	5.30%	False=	4.72%

It is instructive to see what the effect of scanning is. For that purpose the hemispheric cloud mask data of the NubiScope is processed for different zenith angles ranges. Figure 14 shows the frequency distribution per okta interval of the total cloud cover at Cabauw obtained with the NubiScope by evaluating different portions of the sky. The NubiScope value labelled by ZA < x ° denote that the cloudiness is derived for the NubiScope for values of the zenith angles smaller than x °. ZA < 69 ° uses cloud mask from the entire NubiScope scan. The curve denoted by R is the total cloud cover taken from the Results file of the NubiScope. For reference the relative distributions obtained with the LD40 ceilometer at Cabauw by using the METAR and the SYNOP algorithm which use the ceilometer data of a 10-minute and 30-minute interval (the last 10-minutes having double weight), respectively are also shown. Figure 14 indicates that using only the cloud data near the zenith produces low number of situations in the 2 to 6 okta range (about 2 %), the number of cases with 1 and 7 okta is larger (4 and 10 %, respectively), and the number of 0 and 8 okta occur even more often (30 and 40 %, respectively). This "U-shape" distribution is typical for cloud detection

systems covering a small portion of the sky. When a larger portion of the sky is considered the number of occurrences of cases with 1-7 okta gradually increases whereas the 0 and 8 okta decreases. The change of the fraction of occurrence of each okta interval is given more clearly in Figure 15, which shows the same data as Figure 14, but gives the fraction of cases in each okta interval as a function of zenith angle range. The clear sky (n=0) and overcast (n=8) situations gradually decrease with increasing zenith angle range whereas the other curves increase. The curves for 0 and 1 okta show a deviation at the largest zenith angles. At low elevations the NubiScope seems to report clouds too often. If these low elevations are taken into account then the 0 and 1 okta cases undershoot and overshoot the number of cases reported in the Results files. Evidently, the NubiScope performs some internal processing in order to derive the total cloud cover from the cloud mask data.

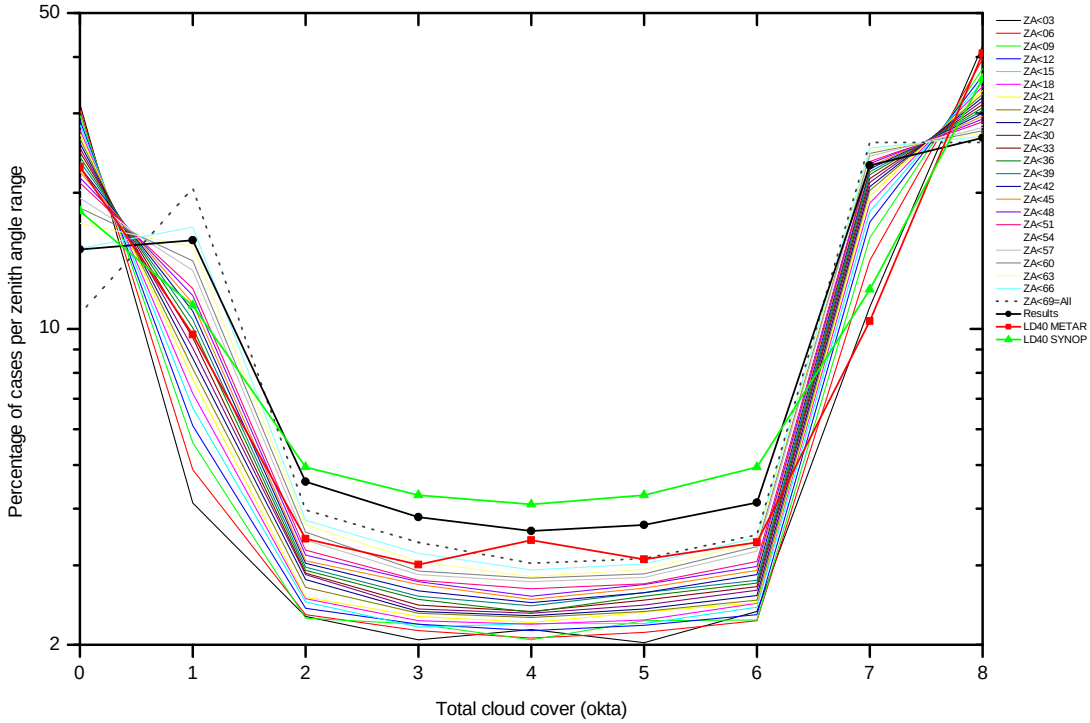

Figure 14: The relative frequency distribution per okta interval of the total cloud cover at Cabauw obtained with the NubiScope by evaluating different portions of the sky.

The LD40 okta distributions show the U-shape as well. The number of cases with 0 and 7 okta is relatively small, the number of 1 to 6 okta is large and the number of 8 okta cases is similar to that of the NubiScope. The large number of 1 to 6 okta situations is partly the result of faulty reports of high clouds during a period when a laser unit with poor quality was employed. Note that increasing the time interval from 10 to 30 minutes in the total cloud cover evaluation for LD40 METAR and SYNOP reduces the number of 0 and 8 okta events and enhances the number of 1-7 okta events.

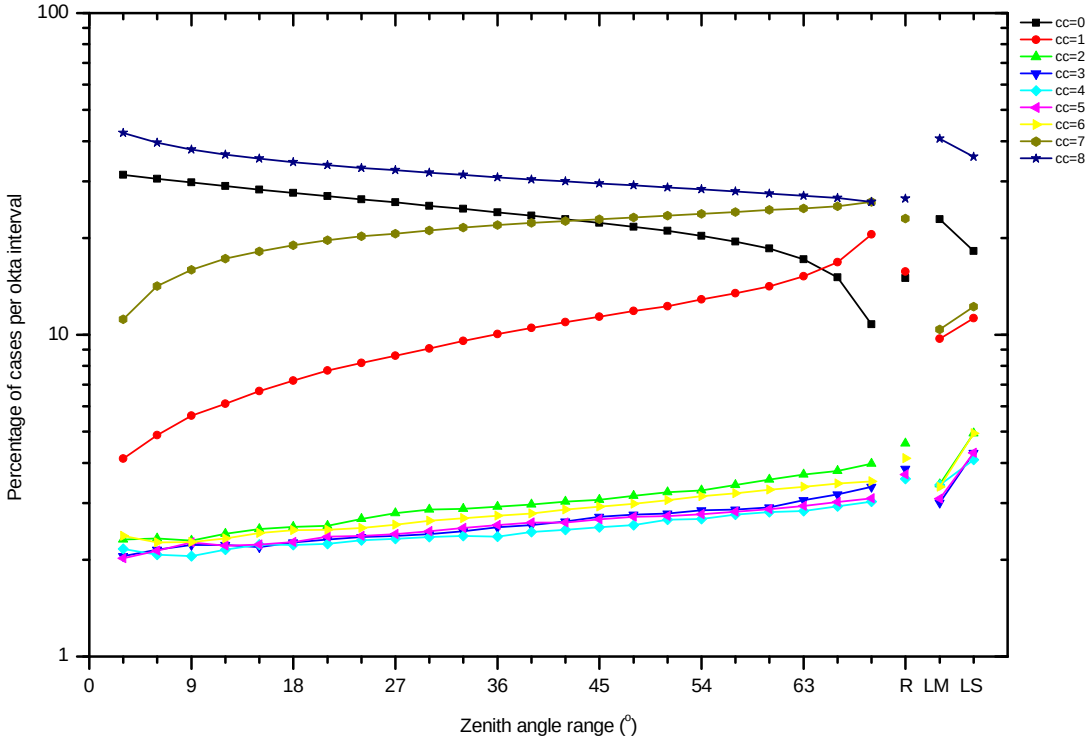

Figure 15: The percentage of cases in each okta interval of the total cloud cover at Cabauw obtained with the NubiScope as a function of the zenith angles range considered. (R=Results, LM=LD40 Metar, LS=LD40 Synop)

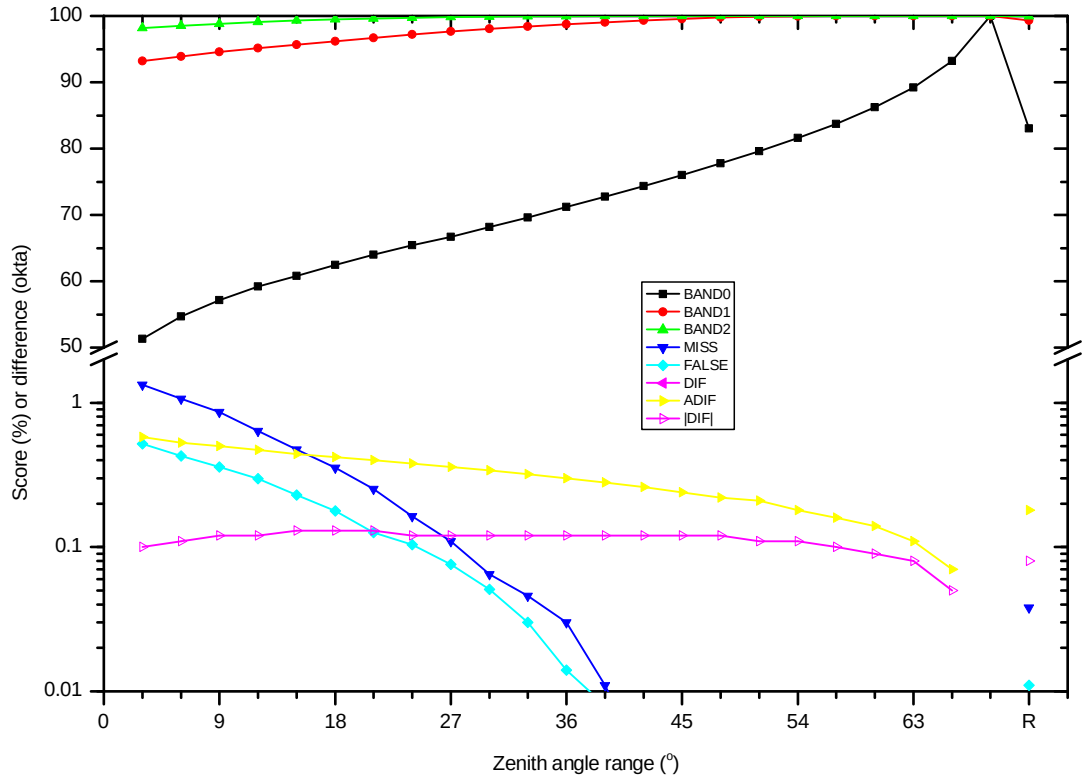

Figure 16: Overall scores and differences when comparing the total cloud cover reported as a function of zenith angle range with the results of obtained from the entire cloud mask.

The differences between the total cloud cover reported by the NubiScope as function of the zenith angles range can also be studied by comparing them with the total cloud cover reported by the NubiScope obtained from the full zenith angle range. For each zenith angles range a contingency matrix can be constructed that gives for each total cloud cover event with a partial zenith angle range that corresponding

total cloud cover of the full zenith angle range. In Figure 16 some scores obtained from the contingency matrices are shown. The scores Band0, Band1 and Band2 are the fraction of cases that the partial and the full zenith angle range total cloud cover are exactly identical (±0 okta), are within ±1 okta, or ±2 okta, respectively. More than 98 % of the cases are always within ±2 okta for each zenith angle range. Band1 contains 93 % of the cases when only the zenith cloud data ZA < 3 ° is used and the scores increases to 95 % at ZA < 12 ° and 98 % at ZA < 30 °. Only 51 % of the cases has identical cloud cover at ZA < 3 ° and improves to 89 % at ZA < 63 ° and 93 % at ZA < 66 °. Clearly a lot of scanning effort is required to obtain a large fraction of identical results. The situation with differences exceeding ±2 okta are classified as either Miss or False when the total cloud cover of the NubiScope for a partial zenith angle range is more than 2 okta less or larger than the NubiScope total cloud cover for the entire zenith angle range. Figure 16 shows that the Miss fraction always exceeds the False fraction because of the increased NubiScope cloudiness at low elevations. The Miss and False fractions are less than 0.1 % at about ZA < 27 ° and below 0.01 % at ZA < 39 °. In addition Figure 16 shows the averaged (absolute) differences in total cloud cover for the partial and full zenith angle scan. The difference is round -0.12 okta and shows little variation with zenith angle range. Only when low elevation are taken, which have on average a larger fraction of clouded pixels, does the difference decrease. The absolute difference is 0.58 okta at ZA < 3 ° and decreases gradually with increasing zenith angle range (0.3 at ZA < 36 °, 0.11 at ZA < 63 °). The above analysis shows the effect of scanning, but it can also be used to design an optimized scanning strategy that meets a full sky scan with some allowed threshold. The above results show that scanning beyond about ZA < 39 ° has little effect on the overall scores. Scanning at lower elevations does however improve the score of Band0 and also affects the total cloud cover distribution.

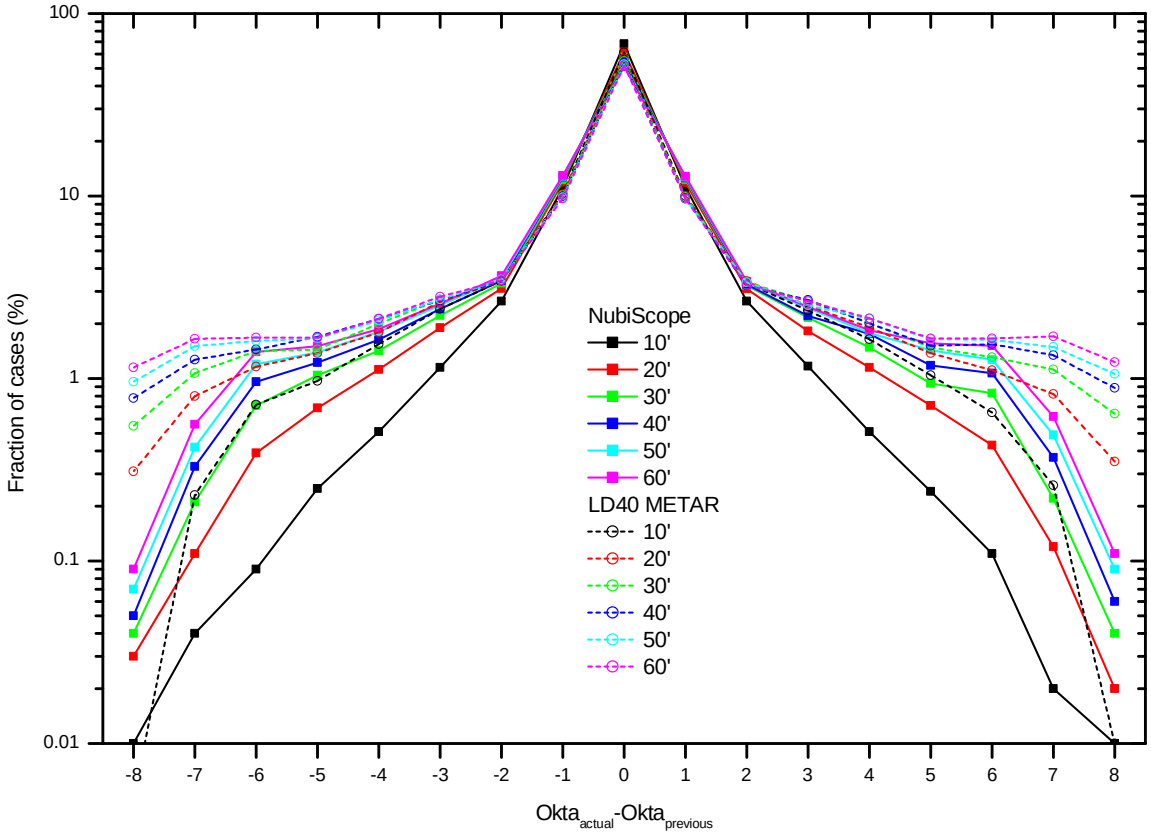

Figure 17: Frequency distribution of differences between the NubiScope and LD40-METAR cloudiness and the cloudiness reported 10 – 60 minutes ago.

Finally the differences between the cloudiness reported at each 10-minute interval are previous intervals are compared. Figure 17 shows the frequency distribution of the differences for NubiScope and LD40-METAR for time intervals 10 to 60 minutes apart. The differences are mostly within ±1 okta. The number of cases with differences larger than ±2 okta increases with increasing time difference. The NubiScope shows fewer cases with differences larger than ±2 okta than LD40-METAR. In fact the distribution of the NubiScope differences at 30-minutes is nearly identical to the LD40-METAR differences at 10-minutes. The fewer cases with differences larger than ±2 okta for NubiScope compared to LD40-METAR also reflects the better spatial representativeness of the first, which reduces the differences between successive cloudiness values.

6. CONCLUSIONS

The NubiScope has been installed at CESAR and operated for more than a year. The pan-and-tilt unit showed problems and has been replaced, but otherwise the NubiScope performed well. The stability and the effect of contamination of the pyrometer have been studied. The deviations from the clean reference show a gradual increase over time. After a year in the field the NubiScope showed differences varying linearly from about +1.8 °C at -40 °C to -0.4 °C at +40 °C. It is not clear if these differences due to contamination are typical and whether it is affected by contamination events or the faulty PTU which sometimes left the NubiScope looking upwards. The absolute calibration of the pyrometer showed deviations of about +2 °C at -40 °C to -0.5 °C at +40 °C over a period of 2 years, the largest part of which occurred prior to the installation at Cabauw. In order to monitor the stability of the pyrometer Heitronics advised to check the pyrometer every 2 month against a black body.

The NubiScope gives a better total cloud cover than the operational KNMI results obtained with a LD40 ceilometer. The NubiScope measurements have better spatial representativeness as a result of scanning. In addition, the NubiScope, as compared to the LD40, is generally more sensitive to middle and high level clouds, although there are also situations when the reverse occurs. As a result of this investigation the Climate department decided to keep the NubiScope permanently at CESAR. The Weather department confirmed the added value of the NubiScope for cloud cover observations, but for applications such as aviation the cloud height information is crucial. The height information derived solely from the NubiScope is by far not as accurate as that obtained with a ceilometer. The combination of NubiScope cloud cover information with accurate height information requires further research.

7. ACKNOWLEDGEMENTS

We are indebted to the KNMI staff that contributed to the evaluation of the NubiScope, in particular Mr. R. van Krimpen for performing the measurements of the pyrometer against the black body radiator, Mr. C. van Oort for the NubiScope data-acquisition, Dr. M. Savenije for constructing the web evaluation tool, Dr. S. de Haan for providing the GPS IWV data, and the observers at Rotterdam Airport for their manual evaluation of the NubiScope cloudiness.

8. REFERENCES

Boers, R., M.J. de Haij, W.M.F. Wauben, H. Klein Baltink, L.H. van Ulft, M. Savenije and C.N. Long (2010), Optimized Fractional Cloudiness Determination from Five Ground - based Remote Sensing Techniques, submitted to J. Geophys. Res.

Collet M., T. Besnard, F. Zanghi, P.W. Chan,L. Berger, C.N Long and D. Gillotay (2009), Improvement of algorithm in cloud thermal infrared spectroscopy, AMS Annual Meeting, Phoenix, Arizona.

Feister, U., H. Möller, T. Sattler, J. Shields, U. Görsdorf and J. Güldner (2010), Comparison of macroscopic cloud data from ground-based measurements using VIS/NIR and IR instruments at Lindenberg, Germany, Atmos. Res. 96, 395-407.

Wauben, W.M.F. (2002), Automation of visual observations at KNMI: (ii) Comparison of automated cloud reports with routine visual observations, AMS Annual Meeting, Orlando, Florida, 2002.

Wauben, W. (2006), Evaluation of the NubiScope, Technical Report No. 291, KNMI, De Bilt.

Wauben, W., H. Klein Baltink, M. de Haij, N. Maat and H. The (2006), Status, Evaluation and new Developments of the Automated Cloud Observations in the Netherlands, IOM 94 (TD 1354) WMO Technical Conference, Geneva, Switzerland.

Wauben, W., M. de Haij, R. Boers, H. Klein Baltink, B. van Ulft and M. Savenije (2010a), On the generation of an optimized fractional cloudiness time series using a multi-sensor approach, WMO-CIMO Technical Conference, paper 2(4), Helsinki.

Wauben, W., F. Bosveld, H. Klein Baltink (2010b), NubiScope Laboratory Tests and Field Evaluation, Technical Report, in preparation, KNMI, De Bilt.